

Fatigue life prediction for threaded joint

A. Krenevičius*, M. Leonavičius**

*Vilnius Gediminas Technical University, Saulėtekio al. 11, 10223 Vilnius, Lithuania, E-mail: kron@fm.vgtu.lt

**Vilnius Gediminas Technical University, Saulėtekio al. 11, 10223 Vilnius, Lithuania, E-mail: minleo@fm.vgtu.lt

1. Introduction

Large equipment such as heat exchangers, steam generators and other pressure vessels are provided with bolted closures for the purpose of in-service inspection and maintenance of internal components. In this case, it is often found that the bolt/stud is the most critical part. In many situations, the studs fail to meet the fatigue requirements for design life of the equipment.

Low fatigue strength of important threaded joints is defined in accordance with the ASME code [1] or Russian Federation standard [2]. These methods require the maximum stress concentration in thread root to be evaluated and this can be done without using a knowledge of the load distribution along the thread helix. However the theoretical prediction of the fatigue life in this way often is difficult. This is because of the effects of load distributions in the thread caused by different structural parameters which are designed in a wide range of dimensions. Trustworthy way for more exact analytical calculation of the stress at the thread roots is direct use of load distribution data. It is unavoidable, when in order to increase cyclic life of threaded joints advanced techniques are used. For example, the data of loads and fatigue damages distribution in thread roots is essential in calculating the fatigue life increase of a threaded connection at periodic change of nut and stud mutual position [3].

In the field of high cycle fatigue a several methods have been suggested to evaluate the fatigue limit of a bolt by employing appropriate theories or empirical laws to calculate the load along the thread helix followed by the maximum stress concentration and then the fatigue limit. The comparison of these methods is performed in [4].

These methods are based on the concept of elastic state of the thread when calculating of load distribution in

the thread and on assumption of limit state of a threaded joint as complete failure of the bolt.

In the case of low cycle loading the distribution of load along the thread helix considerably depends on plastic deformations of the mostly loaded firsts partly and fully engaged turn couples in the threaded joint [5-7]. The analytical method for the calculation of load distribution in thread which evaluates characteristics of elastic-plastic deformation of the turn couples was proposed and developed in [5, 8].

The object of this paper is to assess potential of above-mentioned analytical method in predicting fatigue life of threaded joints by combining this method with standard [2]. For this purpose calculation results have been assessed against fatigue test data which are expressed in terms of numbers of load cycles at fatigue crack initiation in studs/bolts of threaded joints.

2. Distribution of loads and stresses in the thread

Loads over the threaded joints' elements mostly depend on the distribution of load in the turns. This distribution was calculated applying the methods presented in the publications [5, 8], which involve improvement for estimating overload of a threaded joint.

According to this method, a threaded joint shall be divided into five main segments H_i ($i=1-5$), where the turns pliability γ within these segments is either constant or variable Fig 1. Any of the main segments might be divided into some more segments H_{ic} ($c=1-4$), if a specific cross-section appears within this segment, meaning the cross-section where plastic deformation of the turns, of the stud core or of the nut's wall starts to develop.

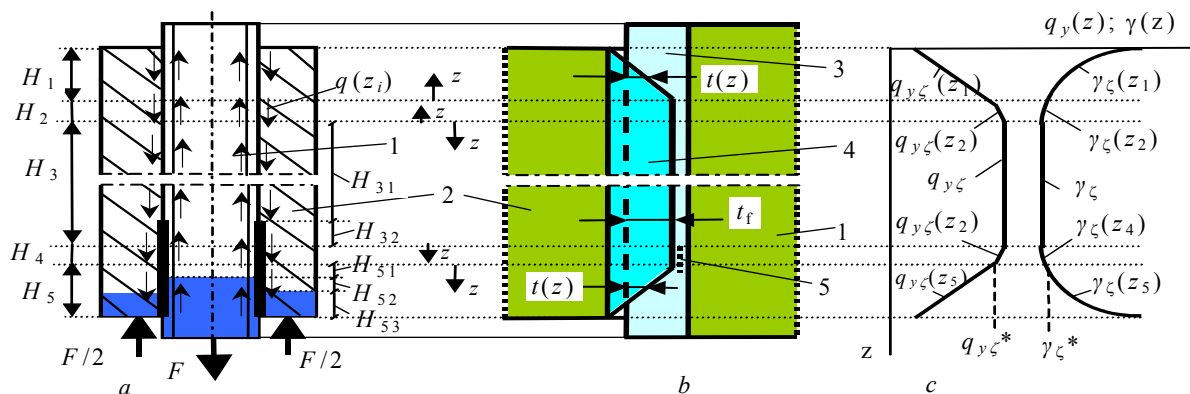


Fig. 1 Threaded joint divided into segments: *a* – segments, *b* – evolvent of engaged turns, *c* – turns' deformation characteristics, 1 – stud; 2 – nut; 3 and 4 – evolvents of engaged stud and nut turns'; 5 - cracks

For instance, in Fig. 1 we see a case, when, due to plastic deformation of the turns, shown by bold line, there appear the segments H_{31} and H_{32} , whereas, at accident of overloading of the threaded joint, due to plastic deformation of the stud core and of the nut's wall, shown as dark areas, there appear the segments H_{51} , H_{52} and H_{53} .

Deformation characteristics the turns of a full or not full profile engagement can be set experimentally, by performing the tensile test of one the couples of turns [5, 8]. Then deformation of turns couples in the threaded joint at any coordinate of contact z_i is expressed as broken turns deformation diagram Fig. 2.

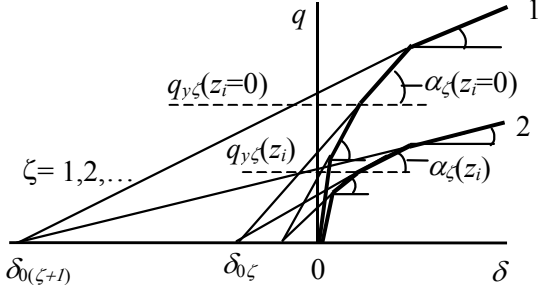


Fig. 2 Deformation diagrams of turn couples: 1 – on boundary of segment, 2 – within segment

One coordinate of this diagram is axial load intensity on turns q , when the other coordinate is the deflection of turns couple δ . Pliability of the turns is $\gamma_\zeta(z_i) = ctg\alpha_\zeta(z_i)$, where the indexes $\zeta = 1, 2, \dots$ define the phases of turns deformation, $q_{y,\zeta}(z_i)$ is yield load intensity of the turns, at which deformation phase ζ begins. In Fig. 2 $\delta_{0,\zeta}$ is constant indices of turns deformation diagram, the first of which is always $\delta_{01} = 0$.

In the middle segment H_3 , where the turns are engaged over the full profile and depth of turns' engagement is t_f (Fig. 1, b). The turns pliability and yield load intensity does not change along all length $\gamma_\zeta(z_3) = \gamma_\zeta = const$ and $q(z_3) = q_y = const$ (Fig. 1, c). In the boundary segments of the joint, i.e. on runouts, where their length is $H_1 = H_5 = P$, due to the changing depth of turns' engagement $t_f(z_i)$ their pliability is varying being $\gamma_\zeta(z_1) = \gamma_\zeta(z_5) \neq const$.

Within the two short transitional segments H_2 and H_4 the turns are engaged over the full profile (Fig. 1, b) but, due to the different boundary conditions their pliability undergoes slight changes here – changes from γ_ζ up to γ_ζ^* (Fig. 1, c). The experiments [9] prove, that fatigue cracks most frequently originate within the segment H_4 .

The system of turns' deformation diagrams (Fig. 2) used here, shows the following characteristics relations for deformation of the turns within segments $i = 1, 2, 4, 5$

$$q_{y,\zeta}(z_i) = \frac{q_{y,\zeta}(0)[\gamma_\zeta(0) - \gamma_{\zeta-1}(0)]}{\gamma_\zeta(z_i) - \gamma_{\zeta-1}(z_i)} \quad (1)$$

$$\delta_{0,\zeta} = q_{y,\zeta}(0)[\gamma_\zeta(0) - \gamma_{\zeta-1}(0)] + \delta_{0(\zeta-1)} \quad (2)$$

where $q_{y,\zeta}(0)$, $\gamma_\zeta(0)$ and $\gamma_{\zeta-1}(0)$ are characteristics of the turns deformation on boundary of a segment at $z_i = 0$.

Now deflection of the turns couple in any segment can be described as follows

$$\delta(z_i) = \gamma_\zeta(z_i)q(z_i) - \delta_{0,\zeta} = \bar{\delta}_\zeta(z_i) - \delta_{0,\zeta} \quad (3)$$

Schematically linear diagram of material's deformation for the stud core is presented on Fig. 3.

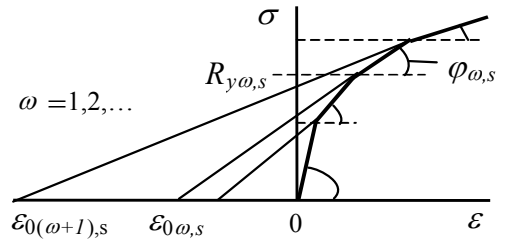


Fig. 3 Deformation diagram of stud material

Material characteristics of the stud are the following: $R_{y\omega,s}$ is stress at the beginning of any material deformation phase ω ; $E_{\omega,s} = tg\varphi_{\omega,s}$ is modulus of the material hardening in deformation phase, ω ; $\epsilon_{0\omega,s}$ are constant indices of material deformation diagram, the first of which is always $\epsilon_{01,s} = 0$. Here $R_{y1,s} = 0$, $R_{y2,s}$ is yield stress, where $R_{pr} < R_{y2,s} < R_{p0.2}$ (R_{pr} , $R_{p0.2}$ - proportional limit and proof strength in real stress-strain curve of the material) and $E_{1,s}$ modulus of elasticity.

The same characteristics apply to the nut's material: $R_{y\varpi,n}$, $E_{\varpi,n}$ and $\epsilon_{0\varpi,n}$, where $\varpi = 1, 2, \dots$ is index of nut's material deformation phase.

The representations, needed to calculate deflections of the turns' and also loads intensity can be obtained by using equation for the displacement compatibility of threaded joints elements'. The equation for a joint with the compressed nut looks as follows [10]

$$\Delta z_{si} + |\Delta z_{ni}| = \delta(z_i) - \delta(0) \quad (4)$$

here Δz_{si} and $|\Delta z_{ni}|$ variations of the stud and nut length in the segment i . Taking into account the fact that the turns' couple, the stud core and the nut wall may get into elastic or elastic-plastic phase of deformation, Eq. (4) can be developed as follows

$$\int_0^z \left[\frac{Q_s(0) + \int_0^z q(z) dz}{E_{\omega,s} A_s} - |\epsilon_{0\omega,s}| \right] dz +$$

$$+\int_0^z \left[\frac{Q_n(0) + \int_0^z q(z) dz}{E_{\omega,n} A_n} - |\varepsilon_{0\omega,n}| \right] dz = \delta(z) - \delta(0) \quad (5)$$

here $z = z_i$, $Q_{s,i}(0)$ and $Q_{n,i}(0)$ are the forces on the stud and nut boundary respectively, according to Fig. 4.

By using Eq. (3) and after differentiation of Eq. (5) two times, the following differential equation was obtained:

$$\bar{\delta}''(z_i) - \left[\frac{\beta_{\omega\sigma}}{\gamma_\zeta(z_i)} \right] \bar{\delta}(z_i) = 0 \quad (6)$$

For the segments, within which pliability of the turns does not change over all length of the segment, i.e. $\gamma_\zeta(z) = \gamma_\zeta = const$ solution of the Eq. (6) is as follows

$$\bar{\delta}(z_i) = A_i sh(m_{\omega\sigma,\zeta} z_i) + B_i ch(m_{\omega\sigma,\zeta} z_i) \quad (7)$$

where $m_{\omega\sigma,\zeta}^2 = \beta_{\omega\sigma} / \gamma_\zeta$; $\beta_{\omega\sigma} = \frac{1}{E_{\omega,s} A_s} + \frac{1}{E_{\omega,n} A_n}$; A_s , A_n are cross-sectional areas of the bolt core and nut wall.

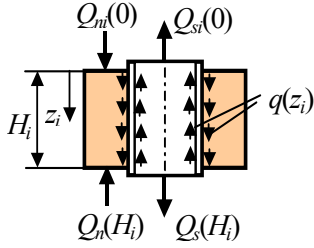


Fig. 4 Boundary conditions on a segment

As in joint segment the deformation of the turns' couple takes place during the first phase $\gamma_\zeta(z_i) = \gamma_1 = const$, while both the bolt and the nut are being under the elastic deformation: $E_{\omega,s} = E_{1s}$, $E_{\omega,n} = E_{1n}$, that is (6) the Birger's differential equation and (7) its solution for defining the load intensity on the turns [10].

In such cases, as in one of the segments the turns' pliability varies, when $\gamma_\zeta(z_i) \neq const$, for the solution of Eq. (6) the next expression has been used

$$\beta_{\omega\sigma} / \gamma_\zeta(z_i) = \Phi^2(z_i) + \Phi'(z_i) \quad (8)$$

where $\Phi(z_i)$ is a selected function, depending on z_i . Then, Eq. (6) can be solved as follows [8]

$$\bar{\delta}(z) = e^{\int_0^z \Phi(z) dz} \left(A_i + B_i \int_0^z e^{-\int_0^z \Phi(z) dz} dz \right) \quad (9)$$

For the turns that are getting out of engagement (concerning segments H_1 and H_5) by using $\Phi(z) = V e^{vz}$ we get the following expression

$$\bar{\delta}(z) = A_i e^{V e^{vz}} + B_i e^{V e^{vz}} \frac{1}{n} \left(\ln t + \frac{t}{1 \cdot 1!} + \frac{t^2}{2 \cdot 2!} + \dots \right) \quad (10)$$

here $t = t(z) = -2 \frac{V}{v} e^{vz}$, $V = V_{\omega\sigma,\zeta}$, $v = v_{\omega\sigma,\zeta}$, $z = z_i$. Fac-

tors $V_{\omega\sigma,\zeta}$ and power exponents $v_{\omega\sigma,\zeta}$ can be defined according to the test results of the turns' couples, engaged over the incomplete profile [8]. They have been defined by using the known turns' pliabilities in one edge of segment H_1 or H_5 where $\gamma_\zeta^* = k_\gamma \gamma_\zeta$ at $z_i = 0$ ($\gamma_\zeta = 1.1$), and also the experimental turns' pliability factors in the middle of the segment $\gamma_1(z_i = H_i/2) = 1.67 \gamma_1$ and $\gamma_2(z_i = H_i/2) = 2.2 \gamma_2$.

In order to solve Eq. (9) with regard to the transitional segments H_2 and H_4 , by using $\Phi(z_i) = U \sin(az_i)$ we get

$$\bar{\delta}(z) = A_i e^{-\frac{U}{a} \cos(az)} + B_i e^{-\frac{U}{a} \cos(az)} \int_0^z e^{\frac{2U}{a} \cos(az)} dz \quad (11)$$

where

$$\begin{aligned} \int_0^z e^{\frac{2U}{a} \cos(az)} dz &= z + \left(\frac{2U}{a} \right) \frac{\sin(az)}{a \cdot 1!} + \\ &+ \left(\frac{2U}{a} \right)^2 \frac{1}{a 2!} \left[\frac{a}{2} z + \frac{1}{4} \sin(2az) \right] + \\ &+ \left(\frac{2U}{a} \right)^3 \frac{1}{a 3!} \left[\sin(az) - \frac{1}{3} \sin^3(az) \right] + \\ &+ \left(\frac{2U}{a} \right)^4 \frac{1}{a 4!} \left[\frac{3a}{8} z + \frac{1}{4} \sin(2az) + \frac{1}{32} \sin(4az) + \dots \right] \\ &+ \left(\frac{2U}{a} \right)^4 \frac{1}{a 4!} \left[\frac{3a}{8} z + \frac{1}{4} \sin(2az) + \frac{1}{32} \sin(4az) + \dots \right] \end{aligned} \quad (12)$$

here $U = U_{\omega\sigma,\zeta}$, $a = a_{\omega\sigma,\zeta}$, $z = z_i$. Factors $U_{\omega\sigma,\zeta}$ and $a_{\omega\sigma,\zeta}$ can be defined by using the already known pliabilities of segment H_2 or H_4 in the edges γ_ζ and γ_ζ^* .

The unknowns: the boundary segments forces $Q_{si}(0) = |Q_{ni}(0)|$ and $Q_s(H_i) = |Q_n(H_i)|$, that are shown in Fig. 4, and factors A_i and B_i of Eqs. (7), (10), (11) are estimated by using the system of equations, which expresses boundary conditions

$$\delta(z_i = H_i) = \delta(z_{i+1} = 0), \quad Q_s(H_i) = Q_{s,i+1}(0) \quad (13)$$

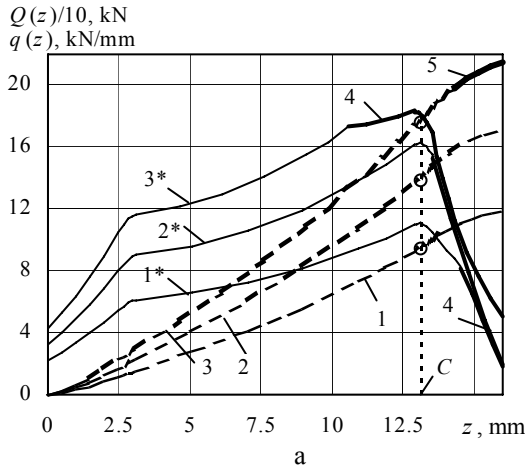
The load intensity $q(z_i)$ of the joint thread turns is defined using Eq. (3). The equation for calculating the stud's core or nut wall's axis force is designed by using the first derivative of Eq. (5)

$$Q(z_i) = Q_i(0) + \int_0^{z_i} q(z_i) dz_i = \beta_{\omega\sigma}^{-1} \left[\delta'(z_i) + |\varepsilon_{0\xi,s}| + |\varepsilon_{0\xi,n}| \right] \quad (14)$$

The alternating maximum local stresses in the thread roots of the stud have been calculated according the formula [11]

$$\sigma_s^*(z_i) = \frac{q(z_i) P}{f} K_m + \frac{Q(z_i)}{A_s} K_0 \quad (15)$$

here K_0 , K_m are concentration factors of the stresses due to the axial force and the stud turn load respectively; f is the turn's contact surface projection into the plane, perpendicular to the stud axis; P is the thread pitch. The values of elastic stress concentration factors, defined in [11] are: $K_0 = 2$ and $K_m = 1.95$, at the turns' root rounding radius



is $R = 0.144P$.

Fig. 5 shows distribution of the loads and of the local stresses in joint M20×2.5, the length thereof being $H = 16$ mm are presented. The parts of the joint are made of steel 25X1MΦ. Mechanical properties of this steel are indicated in Table 1 as steel I. The turn couples, made of this steel, the deformation characteristics are $q_y = 17.3$ kN/mm, $\gamma_1 = 3.78 \times 10^{-3}$ mm/(kN/mm), $\gamma_2 = 12.8 \times 10^{-3}$ mm/(kN/mm). Bold lines 4 of Fig. 5 designate the segment of the joint, in which deformation of the turns takes place under the second nonlinear phase, where $q(z) \geq q_y(z)$, and bold line 5 designates the segment of the joint, where the stud's core is plastically deformed, where $Q(z) \geq R_y A_s$.

Distribution of the local stresses – Fig. 5, b makes it possible to define position of the dangerous section C of the stud z_C as well as the highest local stress $\sigma_s^*(z_C)$, which is used in order to calculate the cyclic life until the moment of formation of the crack in the stud.

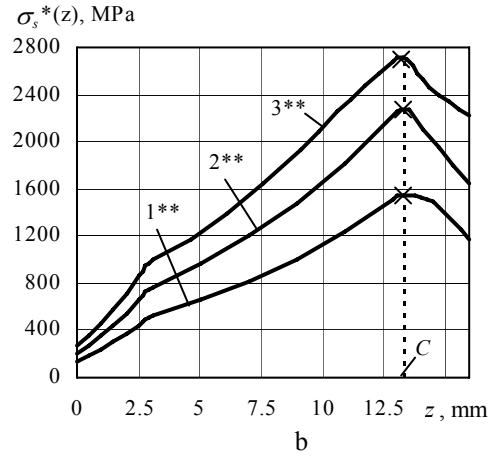


Fig. 5 Distribution of loads (a) and thread root stresses (b) in stud: 1, 2, 3 - $Q(z)$; 1*, 2*, 3* - $q(z)$; 4 - $q(z) > q_y(z)$; 5 - $Q(z) > R_y A_s$; 1, 1*, 1** - $\sigma_s/R_{p0.2} = 0.59$; 2, 2*, 2** - $\sigma_s/R_{p0.2} = 0.85$; 3, 3*, 3** - $\sigma_s/R_{p0.2} = 1.06$

3. Cyclic life of the threaded joints to initiation of the crack

Cyclic life of the studs, prior to origin of the crack N_0 , has been defined in line with the standard [2], using the data, obtained from the distribution of relative elastic stresses (15). Taking into account the fact, that load distribution in the joint is not analysed in the specified norms, we have considered the possibility to apply these data in the standard [2] and verify by comparison of the calculations results with the experimental data.

Two Coffin-Manson-Langer type formulae are presented in standard [2]. The smaller value N_0 has finally been chosen out of two assessed values. These equations applied to the stud, no safety factors considered, are as follows

$$\sigma_{s,a}^* = \frac{E_{1s} e_c}{(4N_0)^m} + \frac{R_{-1}}{1 + (R_{-1}/R_m) \left[\frac{1+r_c}{1-r_c} \right]} \quad (16)$$

$$\sigma_{s,a}^* = \frac{E_{1s} e_c}{(4N_0)^m} + \frac{R_c}{(4N_0)^{m_e} + \left[\frac{1+r_c}{1-r_c} \right]} \quad (17)$$

here R_{-1} is fatigue limit stress of the material, R_m is tensile strength; e_c is material plasticity index, m and m_e are exponents of power, r_c is asymmetry factor of the local stresses cycle, R_c is material strength index.

In this case, $\sigma_{s,a}^*$ is amplitude of conditional maximum local stresses in thread roots of the stud is calculated by using only one stress concentration factor K_σ and at the turns' root rounding radius R , is to be calculated according to the following sequence

$$\sigma_{s,a}^* = K_{ef} \sigma_{s,a}, \quad K_\sigma = 1 + 1.57 \sqrt{P/R} \quad (18)$$

$$R = 0.144P, \quad K_{ef} = K_\sigma$$

and, for flat roots - according to the similar sequence

$$\sigma_{s,a}^* = K_{ef} \sigma_{s,a}, \quad K_\sigma = 1 + 1.57 \sqrt{P/R} \quad (19)$$

$$R = 0.11P, \quad K_{ef} = 1.2K_\sigma$$

where stud nominal stress $\sigma_{s,a}$ is

$$\sigma_{s,a} = F_a / A_s, \quad F_a = (F_{\max} - F_{\min}) / 2 \quad (20)$$

and K_{ef} is effective factor of stress concentration. Other values, employed in the Eqs. (16) and (17), are being assessed according to the following equations

$$R_{-1} = (0.54 - 2 \cdot 10^{-4} R_m) R_m$$

$$e_c = 0.005 Z - (\sigma_{s,\max}^* - R_{p0.2}) / 2E_{1s}$$

when $\sigma_{s,\max}^* > R_{p0.2}$

$$e_c = 0.005 Z, \quad \text{when } \sigma_{s,\max}^* < R_{p0.2}$$

$$m = 0.36 + 2 \cdot 10^{-4} R_m$$

$$R_c = R_m (1 + 1.4 \cdot 10^{-2} Z)$$

and

$$m_e = 0.132 \lg \left[(R_m / R_{-1}) (1 + 1.4 \cdot 10^{-2} Z) \right]$$

here Z is percentage reduction of area of tension specimen, $\sigma_{s,\max}^*$ is maximum conditional elastic stress over the cycle.

By using local stress distribution in the threaded joint, defined under the method presented in Section 2, it is possible to calculate the number of cycles $N_0(z_i)$ until the crack appears for any turn of the stud, as well as for the dangerous section $N_0(z_c) = N_{0C}$ thereof. This option has been analysed in the present work, in order to calculate local stresses according to the formula (15), and for the number of cycles – according to the formula (16), and also according to the adjusted formula (17). So, the cyclic life calculation formulae took the following form

$$\sigma_{s,a}^*(z_c) = \frac{E_{1s} e_c}{[4N_0(z_c)]^m} + \frac{R_{-1}}{1 + \frac{R_{-1}}{R_m} \frac{1+r_c}{1-r_c}} \quad (21)$$

$$\sigma_{s,a}^*(z_c) = \frac{E_{1s} e_c}{[4N_0(z_c)]^m} + \frac{R_c}{[4N_0(z_c)]^{\bar{m}_e} + \frac{1+r_c}{1-r_c}} \quad (22)$$

where the power exponent m_e , adjusted on the basis of the experimental data, received the following expression

$$\bar{m}_e = 0.78(Z10^{-2}) - 0.26(R_m 10^{-3}) \quad (23)$$

To keep the same influence of the thread root rounding as in (18) and (19) the expressions for both stress concentration factors have been designed - for rounded roots

$$K_m = 0.25 + 0.65\sqrt{P/R}$$

$$K_0 = 0.3 + 0.65\sqrt{P/R}, \quad R = 0.144P \quad (24)$$

for flat roots

$$K_m = 1.2(0.25 + 0.65\sqrt{P/R})$$

$$K_0 = 1.2(0.3 + 0.65\sqrt{P/R}), \quad R = 0.11P \quad (25)$$

In the course of analysis aiming to find out whether Eqs. (16), (17) and (24), (25) are appropriate for such an assessment, the calculations data have been compared versus the findings of the threaded joints tests, that had been carrying out for the long time by the authors at the Laboratory of Strength Mechanics of Vilnius Gediminas Technical University.

Mechanical properties of the materials of stud-nut joints (mean values of the characteristics) are given on Table 1. The dimensions of metric thread were as specified by ISO 724. Tests temperature T , K and the number of performed tests are presented in Table 2. Cyclic life tests of the threaded joints have been carried out under axial cyclic loads (as the load is being monitored), the asymmetry coefficients of which were $R = 0; 0.3; 0.6$.

Magnetic luminescent powder method has been employed to define the start point of crack initiation in the stud. Detection of formation of the crack in the stud is being performed on the routine basis by knocking down a joint [9, 12]. After each proof inspection, by using auxiliary nuts with pins, no load applied, the joint is assembled in such a way, that in the course of further testing, position of the nut relative to the stud remains unchanged. Now, such a dangerous state of the stud's thread roots, when the depth of macro crack and the length round the periphery thereof reach (0.1-0.5) mm and (3-6) mm, respectively is considered to be the crack initiation.

In case of threaded joints M20×2.5 made of steel I with the rounded off as well as with the flat roots of the joint, cycling life until the crack formation moment in the dangerous section N_{0C} reached 10^6 load cycles. As an example: Fig. 6 shows the calculated data and also the experimental data for these joints with the flat roots of the thread, the assessment being performed at: $R = 0$. In case of threaded joints M20×2.5 made of steel I with the rounded off as well as with the flat roots of the joint, cycling life

Table 1

Mechanical properties of the materials

Steel	Steel quality	Heat Treatment	T	E	$R_{p0.2}$	R_m	Z
Nr.			K	GPa	MPa	MPa	%
I	25X1MΦ	normalization 1213K, tempering 913K	293	210	900	1020	58.5
II	25X1MΦ	hardening 1486K, tempering 1186K	293	210	950	1100	60.2
II	25X1MΦ	hardening 1486K, tempering 1186K	593	200	847	960	62.5
III	25X1MΦ	hardening 1423K, tempering 1173K	593	200	705	800	63.5
IV	20X1M1Φ1TP	hardening 1526K, tempering 1226K	293	200	820	880	62
IV	20X1M1Φ1TP	hardening 1526K, tempering 1226K	593	200	735	840	63.5
V	38XH3MΦA	hardening 1411K, tempering 1186K	293	210	980	1100	62
V	38XH3MΦA	hardening 1411K, tempering 1186K	593	200	800	950	66
VI	06X13H7I2	hardening 1323K, tempering 823K	293	200	851	996	64.1

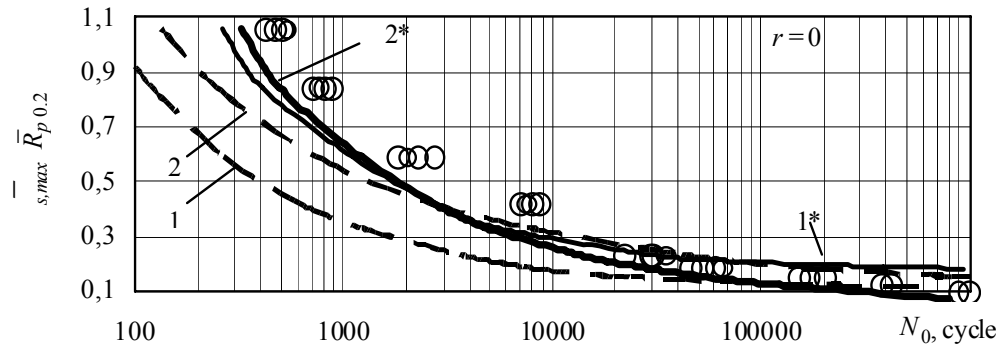


Fig. 6 Fatigue life of threaded joints M20x2.5: 1 - calculation as per formula (16); 2 - calculation as per formula (17); 1* - calculation as per formula (21); 2* - calculation as per formula (22); o – experimental data

until the crack formation moment in the dangerous section N_{0C} reached 10^6 load cycles.

Fig. 6 – it is obvious that curve 2, evaluated according to the specified by the norms formula (16), lies in the safe part of life time range - up to 2×10^4 cycles. Curve 1 is calculated according to the standard [2] formula (17) that is appropriate to be applied over all the life range up to 10^6 cycles, although in the low cycle range with up to 10^4 cycles, the curve is much more remote from experimental points, compared to curve 2. Curves 1* and 2*, estimated according to the modified standard's formulae (21) and (22), fall closer to the experimental points versus the specified curves 1 and 2. In the low cycles range the curves are very close to each other. Curve 1* is suitable for applying within the range of about up to 4×10^4 load cycles and curve 2*, calculated by formula (22) – for applying over the whole range up to 10^6 load cycles. The said curve 2* path in a pretty similar way relates the experimental points, also at the load asymmetries, when $R = 0.3$ and $R = 0.6$, as well as for cases of the rounded thread roots.

Table 2

Tests parameters of the threaded joints

Steel Nr.	T, K	Threaded joint	Number of tests
I	293	M20x2,5	78
I	293	M42x4	6
II	293	M20x2,5	34
II	593	M16x2	32
III	593	M16x2	16
IV	293	M20x2,5	22
IV	593	M16x2	26
V	293	M20x2,5	28
V	593	M16x2	34
VI	293	M16x2	10
VI	293	M42x4	8

The similar way of calculations according to the formula (22), as well as comparison of the experimental' data, have been carried out for the joints with the rounded thread roots, made of steels II - VI and tested at $R = 0; 0.3; 0.6$. Cyclic life of these joints' prior to crack formation reached 5×10^4 load cycles. Fig. 7 and Fig. 8 shows comparison of the cycle life $N_{0C,calc}$, estimated according to formula (22) and in line with the standard [2], with the experimental data $N_{0C,exp}$, obtained at 293 and 593°K.

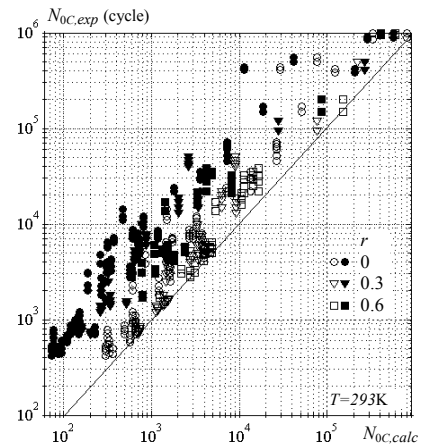


Fig. 7 Lifetime of threaded joints M20x2.5 and M42x4: light points – calculation as per formula (22); black points – as per formula (16 or 17)

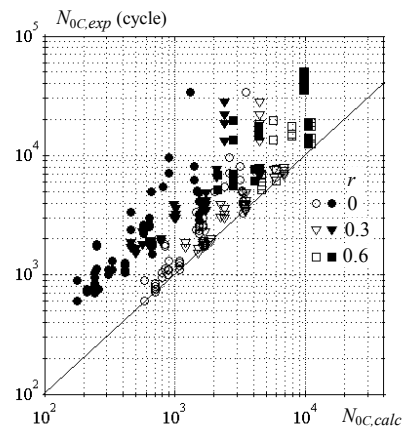


Fig. 8 Lifetime of threaded joints M16x2 at 593K: light points – calculation as per formula (22); black points – as per formula (16 or 17)

Here, it is obvious, that the calculated life characteristic does not exceed the experimental values, whereas the life values, calculated according to formula (22), on the whole, are arranged closer to them, compared to the calculations according to formula (16) or (17).

4. Conclusions

1. To incorporate the threads load distribution data into calculation of cyclic durability of threaded joints the modified Eqs. (21) and (22) could be used. Formula (21) -

in the range of lifetime up to 4×10^4 cycles and formula (22) - up to 10^6 cycles.

2. Low cycle durability up to 4×10^4 cycles of threaded joints set according to modified method for cyclic strength is notably higher (up 3.5 times) than the calculated values set according to the Norm of Russian Federation (Norm RF) [2]. They are close to experimental values, however do not exceed them.

3. In the range of lifetime $4 \times 10^4 - 10^6$ cycles only formulae of Norm RF (17) and modified (22) give the results which do not exceed experimental values in terms of the numbers of load cycles up to crack initiation in the stud or bolt thread. Formula (22) predicts slightly shorter lifetime than that formula (17).

References

1. **ASME Boiler and Pressure Vessel Code, Sec. III.** – Rules for Construction of Nuclear Power Plant Components, Div. I, Subsec. NB, 1995, p.87-92.
2. **Norm for Calculation of Nuclear Power Equipments and Pipelines Strength.** -Moscow: Energoatomizdat, 1989. -525p. (in Russian).
3. **Kreivičius, A., Viskavičius, K., Selivonec, J.** Increasing fatigue durability of bolt joint by variation of nut position. -Mechanika. -Kaunas: Technologija, 2004, Nr.6(50), p.5-11.
4. **Patterson, E.A.** A Comparative study of methods for estimating bolt fatigue limits. -Fatigue and Fracture of Engineering Materials and Structures, 1990, v.13, No1, p.59-81.
5. **Speičys, A., Kreivičius, A.** Load distribution between threads at elastic-plastic deformations.-Mashinovedeniye. -Moscow: Nauka, 1987, Nr.2, p.87-92. (in Russian).
6. **Medekšas, H.** Cyclic strength of notched components. -Mechanika. -Kaunas: Technologija, 2003, Nr.6(44), p.30-36.
7. **Jakušovas, A., Daunys, M.** Strains in crack zones at static and cyclic elastic-plastic deformation. -Mechanika. -Kaunas: Technologija, 2004, Nr.6(50), p.12-17.
8. **Selivonec, J., Kreivičius, A.** Distribution of load in the threads. -Mechanika. -Kaunas: Technologija, 2004, Nr.2(46) p.21-26.
9. **Leonavičius, M., Kreivičius, A.** Shakedown and failure of the threaded joints under low cyclic loading. -J. of Construction Steel Research, 1998, v.46, The Steel Construction Institute. Elsevier, p.452-453.
10. **Birger, I.A., Iosilevich, G.B.** Bolt and Flange Connections. -Moscow: -Mashinostroeniye, 1990. -365p. (in Russian).
11. **Machutov, N.A., Stekolnikov, V.V., Frolov, K.V., Prigorovskij, N.I.** Constructions and Methods of Calculation of Water-Water Power Reactors. -Moscow: Nauka, 1987,-232p. (in Russian).
12. **Jokūbaitis, V.** Regularities in propagation of opened corrosion-induced cracks in concrete. -J. of Civil Engineering and Management. -Vilnius: Technika, 2007, v.13, Nr.2, p.107-113.

A. Kreivičius, M. Leonavičius

SRIEGINIŲ JUNGČIŲ CIKLINIO ILGAAMŽIŠKUMO PROGNOZAVIMAS

R e z i ū m ė

Straipsnyje pateiktas modifikuotas norminis srieginių jungčių ciklinio ilgaamžiškumo prognozavimo metodas, įvertinantis apkrovos pasiskirstymą sriegio vijose. Panaudotas apkrovos ir įtempių pasiskirstymo vijose modelis, kuris atspindi srieginių jungčių medžiagų bei visu ir ne visu profiliu sukibusių vijų porų tempriai plastinio deformavimo savybes. Gauti skaičiavimo rezultatai artimi eksperimentinėms reikšmėms ir jų neviršija.

A. Kreivičius, M. Leonavičius

FATIGUE LIFE PREDICTION FOR THREADED JOINTS

S u m m a r y

This paper presents the modified normative method for threaded joints improved by incorporating in the calculation the data of load distribution in threads. There is used the model for calculation of load and stress distribution along the thread based on elastic plastic deformation properties of the joint materials and full and partial profile turns couples. Results of fatigue life prediction are close to the experimental values, however do not exceed them.

А. Крeнeвичюс, М. Лeонaвичюс

ЦИКЛИЧЕСКАЯ ДОЛГОВЕЧНОСТЬ РЕЗЬБОВЫХ СОЕДИНЕНИЙ

Р e з ю м e

В настоящей работе предложена модификация нормативной методики расчета долговечности резьбовых соединений, учитывающая распределение нагрузки по виткам резьбы. Используется модель распределения нагрузки и напряжений в витках, отражающая свойства упругопластического деформирования материалов соединений и витков при их полном и частичном сопряжении. Полученные результаты расчета по долговечности близки к экспериментальным значениям и их не превышают.

Received February 27, 2008

DOI: 10.5755/j02.mech.15084